

Sleep apnea detection from a single-lead ECG signal with automatic feature-extraction through a modified LeNet-5 convolutional neural network

Tao Wang^{Corresp., 1}, Changhua Lu^{1, 2}, Guohao Shen¹, Feng Hong¹

¹ School of Computer and Information, Hefei University of Technology, Hefei, Anhui, China

² School of Software, Hefei University of Technology, Hefei, Anhui, China

Corresponding Author: Tao Wang

Email address: wtustc@mail.ustc.edu.cn

Sleep apnea (SA) is the most common respiratory sleep disorder, leading to some serious neurological and cardiovascular diseases if left untreated. The diagnosis of SA is traditionally made using Polysomnography (PSG). However, this method requires many electrodes and wires, as well as an expert to monitor the test. Several researchers have proposed instead using a single channel signal for SA diagnosis. Among these options, the ECG signal is one of the most physiologically relevant signals of SA occurrence, and one that can be easily recorded using a wearable device. However, existing ECG signal-based methods mainly use features (i.e. frequency domain, time domain, and other nonlinear features) acquired from ECG and its derived signals in order to construct the model. This requires researchers to have rich experience in ECG, which is not common. A convolutional neural network (CNN) is a kind of deep neural network that can automatically learn effective feature representation from training data and has been successfully applied in many fields. Meanwhile, most studies have not considered the impact of adjacent segments on SA detection. Therefore, in this study, we propose a modified LeNet-5 convolutional neural network with adjacent segments for SA detection. Our experimental results show that our proposed method is useful for SA detection, and achieves better or comparable results when compared with traditional machine learning methods.

1 **Sleep apnea detection from a single-lead ECG signal**
2 **with automatic feature-extraction through a modified**
3 **LeNet-5 convolutional neural network**

4

5 Tao Wang¹, Changhua Lu^{1,2}, Guohao Shen¹, Feng Hong¹

6

7 ¹ School of Computer and Information, Hefei University of Technology, Hefei, Anhui, China

8 ² School of Software, Hefei University of Technology, Hefei, Anhui, China

9

10 Corresponding Author:

11 Tao Wang¹

12 Fuicui Lake Campus of HeFei University of Technology, Hefei, Anhui, China

13 Email address: wtustc@mail.ustc.edu.cn

14

15 **Abstract**

16 Sleep apnea (SA) is the most common respiratory sleep disorder, leading to some serious
17 neurological and cardiovascular diseases if left untreated. The diagnosis of SA is traditionally
18 made using Polysomnography (PSG). However, this method requires many electrodes and wires,
19 as well as an expert to monitor the test. Several researchers have proposed instead using a single
20 channel signal for SA diagnosis. Among these options, the ECG signal is one of the most
21 physiologically relevant signals of SA occurrence, and one that can be easily recorded using a
22 wearable device. However, existing ECG signal-based methods mainly use features (i.e. frequency
23 domain, time domain, and other nonlinear features) acquired from ECG and its derived signals in
24 order to construct the model. This requires researchers to have rich experience in ECG, which is
25 not common. A convolutional neural network (CNN) is a kind of deep neural network that can
26 automatically learn effective feature representation from training data and has been successfully
27 applied in many fields. Meanwhile, most studies have not considered the impact of adjacent
28 segments on SA detection. Therefore, in this study, we propose a modified LeNet-5 convolutional
29 neural network with adjacent segments for SA detection. Our experimental results show that our
30 proposed method is useful for SA detection, and achieves better or comparable results when
31 compared with traditional machine learning methods.

32

33 **Keywords:** Sleep Apnea, ECG, LeNet-5, Convolutional Neural Network, Automatic Feature-
34 Extraction

35

36 Introduction

37 Sleep apnea (SA) is the most common respiratory disorder, caused by partial or complete
38 obstructions of the upper respiratory tract (Li et al. 2018; Punjabi 2008). During sleep, SA events
39 can occur hundreds of times, and, if repeated over a long period of time, can cause serious
40 neurological and cardiovascular complications such as memory loss, high blood pressure,
41 congestive heart failure, and poor cognitive ability during the day (Khandoker et al. 2009; Sharma
42 & Sharma 2016; Varon et al. 2015; Young et al. 1997). Reportedly, approximately 5% of women
43 and 14% of men have SA syndrome in the United States, and the incidence of the disease is
44 increasing in various populations (Peppard et al. 2013; Song et al. 2016). The severity of SA is
45 clinically assessed using the apnea-hypopnea index (AHI). Subjects with an $AHI > 5$ combined
46 with other symptoms (i.e. excessive sleepiness and poor cognitive ability during the day) are
47 diagnosed with SA (Marcus et al. 2012; Song et al. 2016).

48 Polysomnography (PSG) is one of the most common tests used for SA diagnosis. It analyzes
49 physiological signals (e.g. airflow, electroencephalogram (EEG), electrocardiogram (ECG), and
50 respiratory signals) during sleep (Bloch 1997; Song et al. 2016) in a hospital, and requires the
51 patient to wear a number of electrodes and wires while an expert monitors the whole examination
52 process. This complicated and uncomfortable examination experience has limited the application
53 of PSG in clinical practice. To this end, several methods using a single channel signal (i.e. ECG
54 (Penzel et al. 2003), SaQ₂ (Hornero et al. 2007), and respiratory sound (Azarbarzin & Moussavi
55 2013)) for SA diagnosis have been proposed (Song et al. 2016) to reduce costs and to be more
56 easily implemented. Among these, using an ECG signal has been the most popular method because
57 it is one of the most physiologically relevant signals of SA occurrence and can be easily recorded
58 using a wearable device.

59 For example, Song et al. developed a Hidden Markov Model (HMM) SA detection method using
60 the frequency domain and time domain features extracted from EDR signals and ECG signals, and
61 their model achieved an accuracy of 86.2% in per-segment SA detection (Song et al. 2016). Sharam
62 et al. proposed an RBF kernel LS-SVM for the per-segment SA detection based on features
63 extracted from RR intervals by the hermit basic function, and the accuracy of their model was
64 83.8% (Sharma & Sharma 2016). Existing methods mainly use frequency domain, time domain,
65 and some nonlinear features acquired from ECG and its derived signals to construct the model.
66 This requires researchers to have a wealth of relevant domain knowledge and experience,
67 researchers with sufficient experience are uncommon. Recently, Li et al. proposed an SA detection
68 method that uses stacked SAE to automatically extract features (Li et al. 2018). Their method
69 avoids over-reliance on ECG domain knowledge, and achieved an accuracy of 84.7% in per-
70 segment classification. However, stacked SAE is essentially an unsupervised feature

71 transformation that cannot extract features effectively (Kang et al. 2017).
72 A convolutional neural network (CNN) is a deep neural network that simulates the deep hierarchal
73 structure of human vision (Matsugu et al. 2003). Compared to traditional machine learning
74 methods, a CNN does not require hand-crafted features, and can automatically extract effective
75 features through hierarchical layers. It has been successfully applied in speech recognition (Abdel-
76 Hamid et al. 2012; Palaz & Collobert 2015), image classification (Sharif Razavian et al. 2014; Wei
77 et al. 2016), signal analysis (Kwon et al. 2018; Sedighi et al. 2015) and other fields. LeNet-5 is
78 one CNN implementation with relatively few parameters and good performance (El-Sawy et al.
79 2016; LeCun 2015; Wen et al. 2018). It is worth noting that in a CNN, many parameters are prone
80 to overfitting when training small data (i.e. the data used in this study), increasing the difficulty of
81 this task. Therefore, the main objective of this study is to detect SA by automatically extracting
82 features from RR intervals and amplitudes using LeNet-5. Previous studies (De Chazal et al. 2000;
83 Maier et al. 2000; Yadollahi & Moussavi 2009) have shown that adjacent segments offer useful
84 information for SA detection. Additionally, we combine adjacent segments into our proposed
85 method. Experimental results in the PhysioNet Apnea-ECG and UCD datasets show that our
86 proposed method is robust, and its performance has been improved further since, promoting the
87 clinical application of a single-lead ECG SA detection method.

88 **Materials & Methods**

89 **Datasets**

90 To ensure reliable results, two separate datasets were used in this study. A brief description of the
91 two datasets is provided below.

92 *PhysioNet Apnea-ECG dataset*

93 The first dataset was the PhysioNet Apnea-ECG dataset provided by Philipps University
94 (Goldberger et al. 2000; Penzel et al. 2000). It contains a total of 70 single-lead ECG signal
95 recordings (released set: 35 recordings, withheld set: 35 recordings), which were sampled at 100
96 Hz and ranged between 401 and 587 minutes. For each 1-minute ECG signal recording segment,
97 the dataset provided an expert annotation (if there was an apnea event within this minute, it was
98 labeled as SA; otherwise, normal). It was notable that there was no difference between hypopnea
99 and apnea in the provided annotation file, and all events were either obstructive or mixed (central
100 was not included). Additionally, these recordings were classified as Class A, Class B and Class C
101 according to the Apnea–Hypopnea Index (AHI) value. Class A meant that the recording contained
102 10 or more SA segments per hour ($AHI \geq 10$) and the entire recording had at least 100 SA segments.
103 Class B meant that the recording included five or more SA segments per hour ($AHI \geq 5$) and the

104 entire recording contained five to 99 SA segments. Class C (or Normal) meant that the recording
105 had less than five segments of SA per hour ($AHI < 5$).

106 *UCD dataset*

107 The UCD dataset was the second dataset, which was collected by the University College Dublin,
108 and can be downloaded from the PhysioNet website
109 (<https://physionet.org/physiobank/database/ucddb/>). This dataset recorded the complete overnight
110 PSG recordings of 25 (4 females and 21 males) suspected sleep disordered breathing patients, each
111 contained 5.9 to 7.7 hours of ECG signal as well as an annotation of the start time and the duration
112 of every apnea/hypopnea event. Considering that this study primarily performed SA detection on
113 1-minute ECG signal segments, we converted continuous ECG data to 1-minute intervals which
114 we correlated with annotations for normal and apnea events. According to the definition of apnea,
115 an event should last at least 10s. However, an apnea event lasting 10s may be separated over two
116 adjacent minutes, each having a smaller amount of apnea event time (Mostafa et al. 2018; Xie &
117 Minn 2012). In the case of apnea or hypopnea lasting 5 or more consecutive seconds, the minute
118 is considered to be an apnea. Additionally, each recording was classified as Class A, Class B or
119 Class C by the Apnea–Hypopnea Index (AHI) value.

120 **Preprocessing**

121 A method for automatically extracting features from RR intervals and amplitudes was developed
122 in this study, and a preprocessing scheme was needed in order to obtain the RR intervals and
123 amplitudes. Since several studies (De Chazal et al. 2000; Maier et al. 2000; Yadollahi & Moussavi
124 2009) have shown that adjacent segment information is helpful for per-segment SA detection, the
125 labeled segment and its surrounding ± 2 segments of the ECG signal (five 1-minute segments in
126 total) were all extracted for processing. We first used the Hamilton algorithm (Hamilton 2002) to
127 find the R-peaks, then used the position of the R-peaks to calculate the RR intervals (distance
128 between R-peaks) and extract the values of the R-peaks (amplitudes). Considering that the
129 extracted RR intervals had some physiologically uninterpretable points, the median filter proposed
130 by Chen et al. (Chen et al. 2015) was employed. Since the obtained RR intervals and amplitudes
131 were not equal time intervals, which was required by our proposed method, cubic interpolation
132 was further employed, and 900 points of RR intervals and 900 points of amplitudes over 5-minute
133 segments were obtained. The detailed preprocessing scheme is shown in Figure 1.

134 **Convolutional Neural Network**

135 In recent years, a CNN has been used as a research hotspot in the field of artificial intelligence
136 (AI). It is a deep neural network method that simulates the deep hierarchal structure of human

137 vision and has been successfully applied in image classification, natural language processing
 138 (NLP) and speech recognition (Palaz & Collobert 2015; Sharif Razavian et al. 2014; Yin et al.
 139 2017). Due to its proficiency in automatic feature extraction, CNN is also used to design advanced
 140 signal analysis methods (Kwon et al. 2018; Sedighi et al. 2015). For example, (Kiranyaz et al.
 141 2015) used CNN for ECG classification. Here, we used a simple and effective CNN
 142 implementation, LeNet-5, to construct our SA detection model. In the following section, we will
 143 introduce both the standard LeNet-5 and our modified LeNet-5.

144 *Architecture of the standard LeNet-5*

145 The standard LeNet-5 proposed by LeCun et al. (LeCun 2015) was designed to solve the problem
 146 of character recognition. It consisted of an input layer, two convolution layers, two fully connected
 147 layers, two pooling layers and an output layer -- in total, seven layers. The details of each layer are
 148 described in (LeCun 2015). Formally, a set of N images $\{X_i, y_i\}_{i=1}^N$ are taken, where X_i is the original
 149 image data and y_i is a class category of the image (i.e. 0 and 1). The difference between the
 150 predicted label \hat{y}_i and the real label y_i is calculated using the categorical cross entropy function,
 151 defined as follows:

$$152 \quad J(\omega, b) \triangleq -\frac{1}{N} \sum_{l=1}^N y_{l1} \log \hat{y}_{l1} + \dots + y_{lK} \log \hat{y}_{lK}$$

153 where ω and b represent the weights and biases of the standard LeNet-5 network layers,
 154 respectively. K is the number of class category and \hat{y}_{lk} corresponds to the softmax value of the k 'th
 155 class category, defined as:

$$156 \quad \hat{y}_{lk} = \text{softmax}(z_k) = \frac{e^{z_k}}{\sum_{i=1}^K e^{z_i}}$$

157 where z_i is the result of the corresponding i 'th class category of the last fully connected output.
 158 The weight and bias parameters of the convolutional operation and fully connected layers were
 159 learned by back-propagating (BP) the derivative of the loss with respect to parameters throughout
 160 the entire network (Zeiler & Fergus 2014).

161 *Architecture of our modified LeNet-5*

162 Unlike with character recognition, the time series used in this study had one-dimensional data,
 163 which is significantly different from two-dimensional character recognition problems. When

164 compared with the millions of training samples in the field of character or image classification, the
165 data samples used in this study were smaller, which increases the risk of overfitting. Moreover,
166 SA detection is a binary classification problem that differs from character recognition. The feature
167 maps, convolution layer strides and fully-connected layer nodes in the standard LeNet-5 may not
168 be suitable for this scene. Therefore, we adjusted LeNet-5 as follows: 1) using a one-dimensional
169 convolution operation instead of a two-dimensional convolution operation to feature extraction
170 (Kiranyaz et al. 2015) ; 2) adding a dropout layer between the convolution layer and fully
171 connected layer to avoid over-fitting (Srivastava et al. 2014); 3) retaining only one fully connected
172 layer to reduce network complexity (Ma et al. 2018); 4) modifying the size of the convolution
173 layer strides and the number of fully-connected layer nodes. The architecture and details of our
174 modified LeNet-5 are shown in Figure 2 and Table 1, respectively. Compared to the standard
175 LeNet-5, all convolution layer strides of our modified LeNet-5 were changed to two, and the
176 number of feature maps was increased layer by layer. In particular, a dropout layer with a drop
177 rate of 0.8 was added between the convolution layer and the fully connected layer, and the number
178 of output layer nodes was reduced from 10 to two for our binary classification problem.

179 **Experiment settings**

180 In the field of SA detection based on a single-lead ECG signal, existing methods mainly extract
181 suitable features based on expert experience, and then construct a model using the extracted
182 features (Sharma & Sharma 2016; Song et al. 2016; Varon et al. 2015), a process called feature
183 engineering. In order to evaluate the performance of our proposed method, several popular feature
184 engineering-based machine learning methods, including Support Vector Machine (SVM), K-
185 Nearest Neighbor (KNN), Logistic Regression (LR) and Multi-Layer Perception (MLP), were
186 employed for comparison. Various features that might have provided useful information for SA
187 detection had been built in previous studies, and here we employed the features (RR intervals: 12
188 features, amplitudes: six features) that had an important effect on SA detection (De Chazal et al.
189 2000; Song et al. 2016) as the input of feature engineering-based methods. Table 2 lists the details
190 of these features. Since some methods are sensitive to feature scales (i.e. KNN), the min-max
191 normalization was used to normalize all features, which is defined as follows:

$$192 \quad x^* = \frac{x - x_{min}}{x - x_{max}}$$

193 where x is the feature to be normalized, and x_{max} and x_{min} are the maximum and minimum value
194 in the features, respectively.

195 **Evaluation**

196 By following (Song et al. 2016; Varon et al. 2015), the specificity (Sp), sensitivity (Sn), accuracy
197 (Acc) and area under the curve (AUC) were employed to evaluate the performance of our proposed
198 method, defined as follows:

$$199 \quad \text{specificity} = \frac{TN}{TN + FP}$$

$$200 \quad \text{sensitivity} = \frac{TP}{TP + FN}$$

$$201 \quad \text{accuracy} = \frac{TP + TN}{TP + TN + FP + FN}$$

202 where *FP* and *TP* stand for “false positive” and “true positive”, respectively. *FN* and *TN* represent
203 “false negative” and “true negative”, respectively.

204 **Results & Discussion**

205 In this study, two separate datasets were used to validate our proposed method. The PhysioNet
206 Apnea-ECG dataset was used as benchmark data to evaluate our proposed method’s performance.
207 The UCD dataset is an independent dataset we used to check the robustness of our proposed
208 method against other datasets.

209 **Per-segment SA detection**

210 Accurately predicting the presence of SA by given ECG segment (minute-by-minute) is key in this
211 field, as it provides a solid foundation for the diagnosis of suspected SA patients. Therefore, we
212 compared our proposed method with traditional machine learning methods on per-segment SA
213 detection. The overall performance of the withhold set, including its specificity, sensitivity,
214 accuracy and AUC, was used for comparison, as displayed in Table 3. As can be seen from Table
215 3, our modified LeNet-5 with automatic feature extraction performed well in all measurements
216 with a specificity of 90.3%, sensitivity of 83.1%, accuracy of 87.6% and AUC of 0.950. Compared
217 with the SVM that had the second highest accuracy, the overall performances were better by 6.0%,
218 6.2%, 6.2% and 0.063, respectively. It can also be seen from the results that KNN had the lowest
219 prediction accuracy among the five methods, probably because the features extracted from the
220 ECG signal were less spatially correlated and were not suitable for this scene, similar to the
221 findings in literature (Sharma & Sharma 2016). In summary, in per-segment SA detection, our
222 proposed LeNet-5 with automatic feature extraction performed better than the commonly used
223 feature engineering method.

224 **Per-recording classification**

225 A recording consists of multiple one-minute ECG segments, and the classification of each
226 recording refers to the overall SA diagnosis of these one-minute ECG segments, which is different
227 from per-segment SA detection. Clinically, AHI is used to distinguish SA from normal recordings.
228 Specifically, if the recording AHI is greater than 5, it is diagnosed as SA; otherwise it is considered
229 to be normal. The recording AHI is calculated using the results of per-segment SA detection, which
230 is defined as follows:

$$231 \quad AHI = \frac{60}{T} * num\ of\ OSA\ segments$$

232 Where T denotes the number of one-minute ECG segment signals, and $T/60$ is the hour of the entire
233 recording. Therefore, AHI is employed here to diagnose the recording SA, and the above-
234 mentioned measurement's accuracy, sensitivity, specificity and AUC are computed on the
235 withheld set as listed in Table 4. It should be noted that the withheld set provided by the PhysioNet
236 Apnea-ECG dataset had only 35 recordings, which may have resulted in low-precision per-
237 segment methods showing better per-recording performance. By following previous studies
238 (Sharma & Sharma 2016; Song et al. 2016), the correlation value between the experimentally
239 determined AHI and the actual AHI were also adopted to ensure the reliability of the comparison.
240 As shown in Table 4, when compared with SVM, LR, KNN and MLP, our modified LeNet-5 with
241 an accuracy of 97.1%, sensitivity of 100%, specificity of 91.7% and AUC of 0.996 performed
242 better in per-recording classification. The correlation value of our modified LeNet-5 further
243 confirmed this result, which increased by 0.091 when compared to the second highest SVM
244 method.

245 **Effect of automatic feature extraction**

246 In the previous parts, we discussed the overall performance of our proposed LeNet-5 in per-
247 recording classification and per-segment detection. The results showed that, when compared with
248 the existing methods, our proposed method significantly improved the performance in both per-
249 recording classification and per-segment SA detection. Here, we will verify the power of the
250 automatic feature extraction of our proposed method. Figure 3 displays the receiver operating
251 characteristic (ROC) curves of our modified LeNet-5 and MLP in per-segment SA detection, since
252 our modified LeNet-5 can be seen as a combination of convolutional neural networks (CNN) for
253 feature extraction and full connection (FC, also known as MLP) as classifier (Bae et al. 1998;
254 Ludermir et al. 2006), meaning that the effects of the automatic extraction features obtained by
255 our proposed LeNet-5 and the features extracted by traditional feature engineering can be directly
256 compared. As shown in Figure 3, the LeNet-5's ROC curve is always above the MLP's ROC
257 curve. These results suggest that the effect of the features extracted by our proposed automatic

258 feature extraction method easily exceeded traditional feature engineering. Additionally, the
259 measurements of the two methods in Table 3 also verify this result.

260 **Robustness Evaluation**

261 *Ten-fold cross-validation*

262 Validating a method with a single small-size test dataset may be biased or lead to incorrect results
263 (Sharma & Sharma 2016; Song et al. 2016). To this end, we used ten-fold cross-validation to
264 ensure that our proposed method was robust under different test datasets. The whole dataset (70
265 recordings) was randomly split into 10 groups, of which nine were adopted to train the classifiers
266 (SVM, LR, KNN, MLP and LeNet-5), and the remaining one was used for the test, taken 10 times.
267 The accuracy of the per-segment SA detection calculated on 10 different test groups was drawn
268 and is shown in Figure 4. As seen in Figure 4, the accuracies obtained using the SVM, LR, KNN,
269 MLP and LeNet-5 ranged from 71.9% to 88.6% (mean \pm standard deviation, $81.1\% \pm 5.50\%$),
270 71.7% to 87.8% (mean \pm standard deviation, $80.6\% \pm 5.47\%$), 72.5% to 84.8% (mean \pm standard
271 deviation, $79.3\% \pm 4.53\%$), 75.4% to 89.9% (mean \pm standard deviation, $81.9\% \pm 4.98\%$) and
272 84.2% to 93.7% (mean \pm standard deviation, $88.7\% \pm 3.05\%$), respectively. These results suggest
273 that our proposed LeNet-5 with automatic feature extraction was more robust, and could achieve
274 consistent and significantly better performances in different test datasets.

275 *Validation on UCD database*

276 To ensure that our proposed method was robust in other datasets, we tested the performance of our
277 modified LeNet-5 on an independent UCD dataset. Similar to the PhysioNet Apnea-ECG dataset,
278 the dataset was divided into two parts, one for training and the other for verification. It is
279 noteworthy that the original UCD dataset is continuously annotated based on the occurrence of
280 events, which is different from the PhysioNet Apnea-ECG dataset, and we followed (Mostafa et
281 al. 2018; Xie & Minn 2012) in converting them to 1-minute interval annotations. Table 5 shows
282 the performance of our modified LeNet-5 and traditional machine learning methods in per-segment
283 SA detection and per-recording classification. As shown in Table 5, the overall performance of
284 different methods on the UCD dataset was worse than that of the PhysioNet dataset, caused by the
285 small number of SA annotations on the UCD dataset. However, our modified LeNet-5 still had
286 better or comparable performance to the traditional machine learning methods. For example, when
287 compared with SVM in per-segment SA detection, the accuracy of our modified LeNet-5 was
288 1.2% better. In per-recording classification, our modified LeNet-5 had the same accuracy as SVM,
289 but the correlation increased by 0.373. In general, our modified LeNet-5 is useful for SA detection.

290 **Comparison with existing works**

291 So far, several works on SA detection based on a single-lead ECG signal have been published in
292 the literature, and these works are mainly focused on feature engineering. Here, we compared our
293 proposed method with relevant work that used both withheld sets and released sets of the
294 PhysioNet Apnea-ECG dataset. However, a direct comparison was not available, due to the
295 different samples sizes (Li et al. 2018). Table 6 shows the relevant work and performance of using
296 the same dataset for per-segment detection. The released set was used for training, and the withheld
297 set was used for validation. As shown, the classification accuracy of existing works ranged from
298 83.4% to 86.2%, which is lower than our proposed method (with an accuracy of 87.6%). It should
299 be noted that Li et al. obtained the best sensitivity since their work is based on sensitivity
300 optimization, while other works have focused on optimizing total classification accuracy (Li et al.
301 2018). Table 7 lists the relevant pre-recording classification work and performance in which the
302 same dataset is employed. It is noteworthy that, as we mentioned above, using traditional
303 measurements to evaluate performance is not very accurate due to relatively small sample size
304 (only 35 recordings in the withheld dataset), and the best method is to take the correlation value
305 between the experimentally determined *AHI* and the actual *AHI* together, but not all works provide
306 the correlation value. Nonetheless, our proposed method, with an accuracy of 97.1%, provides
307 better or comparable performance than these works presented in the literature.

308 **Conclusions**

309 In this study, we developed an SA detection method based on modified LeNet-5 and adjacent ECG
310 segments. Experimental results showed that our proposed method is useful for SA detection, and
311 the performance of our method is better than both traditional machine learning methods and
312 existing works. Due to the high precision requirements of clinical applications, further
313 improvements in our proposed method will accelerate the development of ECG-based SA
314 detection devices in clinical practice. Furthermore, since only a single-lead ECG signal is used,
315 our proposed method can also be used to develop SA detection for home healthcare services using
316 wearable devices. However, our proposed method has some limitations. Because the Apnea-ECG
317 dataset is labeled in 1-minute segments, an apnea/hypopnea event could occur in the middle of two
318 1-minute segments and a 1-minute segment could contain more than one apnea/hypopnea event.
319 Additionally, the dataset does not separately label hypopnea and apnea events in the provided
320 annotation file, and all events are either obstructive or mixed (central is not included). This could
321 mean our proposed method cannot distinguish between hypopnea and apnea, and cannot detect
322 central events. In future research, we will include other datasets to solve the above problems.

323 **Acknowledgements**

324 The authors would like to thank Dr. Thomas for providing the data.

325 **References**

- 326 Abdel-Hamid O, Mohamed A-r, Jiang H, and Penn G. 2012. Applying convolutional neural
327 networks concepts to hybrid NN-HMM model for speech recognition. 2012 IEEE
328 international conference on Acoustics, speech and signal processing (ICASSP): IEEE. p
329 4277-4280.
- 330 Azarbarzin A, and Moussavi Z. 2013. Snoring sounds variability as a signature of obstructive sleep
331 apnea. *Medical engineering & physics* 35:479-485.
- 332 Bae JH, Jung KC, Kim JW, and Kim HJ. 1998. Segmentation of touching characters using an
333 MLP. *Pattern Recognition Letters* 19:701-709.
- 334 Bloch KE. 1997. Polysomnography: a systematic review. *Technology and health care* 5:285-305.
- 335 Chen L, Zhang X, and Song C. 2015. An automatic screening approach for obstructive sleep apnea
336 diagnosis based on single-lead electrocardiogram. *IEEE Transactions on Automation
337 Science and Engineering* 12:106-115.
- 338 De Chazal P, Heneghan C, Sheridan E, Reilly R, Nolan P, and O'Malley M. 2000. Automatic
339 classification of sleep apnea epochs using the electrocardiogram. *Computers in Cardiology
340 2000 Vol 27 (Cat 00CH37163): IEEE. p 745-748.*
- 341 El-Sawy A, Hazem E-B, and Loey M. 2016. CNN for handwritten arabic digits recognition based
342 on LeNet-5. *International Conference on Advanced Intelligent Systems and Informatics:*
343 *Springer. p 566-575.*
- 344 Goldberger AL, Amaral LA, Glass L, Hausdorff JM, Ivanov PC, Mark RG, Mietus JE, Moody
345 GB, Peng C-K, and Stanley HE. 2000. PhysioBank, PhysioToolkit, and PhysioNet:
346 components of a new research resource for complex physiologic signals. *Circulation
347 101:e215-e220.*
- 348 Hamilton PS. 2002. Open source ECG analysis software documentation. *Computers in cardiology
349 2002:101-104.*
- 350 Hornero R, Álvarez D, Abásolo D, del Campo F, and Zamarron C. 2007. Utility of approximate
351 entropy from overnight pulse oximetry data in the diagnosis of the obstructive sleep apnea
352 syndrome. *IEEE Transactions on Biomedical Engineering* 54:107-113.
- 353 Kang M, Ji K, Leng X, Xing X, and Zou H. 2017. Synthetic aperture radar target recognition with
354 feature fusion based on a stacked autoencoder. *Sensors* 17:192.
- 355 Khandoker AH, Palaniswami M, and Karmakar CK. 2009. Support vector machines for automated
356 recognition of obstructive sleep apnea syndrome from ECG recordings. *IEEE transactions
357 on information technology in biomedicine* 13:37-48.

- 358 Kiranyaz S, Ince T, and Gabbouj M. 2015. Real-time patient-specific ECG classification by 1-D
359 convolutional neural networks. *IEEE Transactions on Biomedical Engineering* 63:664-
360 675.
- 361 Kwon Y-H, Shin S-B, and Kim S-D. 2018. Electroencephalography based fusion two-dimensional
362 (2D)-convolution neural networks (CNN) model for emotion recognition system. *Sensors*
363 18:1383.
- 364 LeCun Y. 2015. LeNet-5, convolutional neural networks. URL: <http://yann.lecun.com/exdb/lenet>
365 20.
- 366 Li K, Pan W, Li Y, Jiang Q, and Liu G. 2018. A method to detect sleep apnea based on deep neural
367 network and hidden markov model using single-lead ECG signal. *Neurocomputing* 294:94-
368 101.
- 369 Ludermir TB, Yamazaki A, and Zanchettin C. 2006. An optimization methodology for neural
370 network weights and architectures. *IEEE Transactions on Neural Networks* 17:1452-1459.
- 371 Ma M, Gao Z, Wu J, Chen Y, and Zheng X. 2018. A Smile Detection Method Based on Improved
372 LeNet-5 and Support Vector Machine. 2018 IEEE SmartWorld, Ubiquitous Intelligence &
373 Computing, Advanced & Trusted Computing, Scalable Computing & Communications,
374 Cloud & Big Data Computing, Internet of People and Smart City Innovation
375 (SmartWorld/SCALCOM/UIC/ATC/CBDCOM/IOP/SCI): IEEE. p 446-451.
- 376 Maier C, Bauch M, and Dickhaus H. 2000. Recognition and quantification of sleep apnea by
377 analysis of heart rate variability parameters. *Computers in Cardiology 2000 Vol 27 (Cat*
378 *00CH37163)*: IEEE. p 741-744.
- 379 Marcus CL, Brooks LJ, Ward SD, Draper KA, Gozal D, Halbower AC, Jones J, Lehmann C,
380 Schechter MS, and Sheldon S. 2012. Diagnosis and management of childhood obstructive
381 sleep apnea syndrome. *Pediatrics* 130:e714-e755.
- 382 Matsugu M, Mori K, Mitari Y, and Kaneda Y. 2003. Subject independent facial expression
383 recognition with robust face detection using a convolutional neural network. *Neural*
384 *Networks* 16:555-559.
- 385 Mostafa SS, Morgado-Dias F, and Ravelo-García AG. 2018. Comparison of SFS and mRMR for
386 oximetry feature selection in obstructive sleep apnea detection. *Neural Computing and*
387 *Applications*:1-21.
- 388 Palaz D, and Collobert R. 2015. Analysis of cnn-based speech recognition system using raw speech
389 as input. *Idiap*.
- 390 Penzel T, Kantelhardt JW, Grote L, Peter J-H, and Bunde A. 2003. Comparison of detrended
391 fluctuation analysis and spectral analysis for heart rate variability in sleep and sleep apnea.
392 *IEEE Transactions on Biomedical Engineering* 50:1143-1151.
- 393 Penzel T, Moody GB, Mark RG, Goldberger AL, and Peter JH. 2000. The apnea-ECG database.

- 394 Computers in Cardiology 2000 Vol 27 (Cat 00CH37163): IEEE. p 255-258.
- 395 Peppard PE, Young T, Barnet JH, Palta M, Hagen EW, and Hla KM. 2013. Increased prevalence
396 of sleep-disordered breathing in adults. *American journal of epidemiology* 177:1006-1014.
- 397 Punjabi NM. 2008. The epidemiology of adult obstructive sleep apnea. *Proceedings of the*
398 *American Thoracic Society* 5:136-143.
- 399 Sedighi B, Palit I, Hu XS, Nahas J, and Niemier M. 2015. A CNN-inspired mixed signal processor
400 based on tunnel transistors. 2015 Design, Automation & Test in Europe Conference &
401 Exhibition (DATE): IEEE. p 1150-1155.
- 402 Sharif Razavian A, Azizpour H, Sullivan J, and Carlsson S. 2014. CNN features off-the-shelf: an
403 astounding baseline for recognition. Proceedings of the IEEE conference on computer
404 vision and pattern recognition workshops. p 806-813.
- 405 Sharma H, and Sharma K. 2016. An algorithm for sleep apnea detection from single-lead ECG
406 using Hermite basis functions. *Computers in biology and medicine* 77:116-124.
- 407 Song C, Liu K, Zhang X, Chen L, and Xian X. 2016. An obstructive sleep apnea detection
408 approach using a discriminative hidden Markov model from ECG signals. *IEEE*
409 *Transactions on Biomedical Engineering* 63:1532-1542.
- 410 Srivastava N, Hinton G, Krizhevsky A, Sutskever I, and Salakhutdinov R. 2014. Dropout: a simple
411 way to prevent neural networks from overfitting. *The Journal of Machine Learning*
412 *Research* 15:1929-1958.
- 413 Varon C, Caicedo A, Testelmans D, Buyse B, and Van Huffel S. 2015. A novel algorithm for the
414 automatic detection of sleep apnea from single-lead ECG. *IEEE Transactions on*
415 *Biomedical Engineering* 62:2269-2278.
- 416 Wei Y, Xia W, Lin M, Huang J, Ni B, Dong J, Zhao Y, and Yan S. 2016. HCP: A flexible CNN
417 framework for multi-label image classification. *IEEE transactions on pattern analysis and*
418 *machine intelligence* 38:1901-1907.
- 419 Wen L, Li X, Gao L, and Zhang Y. 2018. A new convolutional neural network-based data-driven
420 fault diagnosis method. *IEEE Transactions on Industrial Electronics* 65:5990-5998.
- 421 Xie B, and Minn H. 2012. Real-time sleep apnea detection by classifier combination. *IEEE*
422 *transactions on information technology in biomedicine* 16:469-477.
- 423 Yadollahi A, and Moussavi Z. 2009. Acoustic obstructive sleep apnea detection. 2009 annual
424 international conference of the IEEE engineering in medicine and biology society: IEEE.
425 p 7110-7113.
- 426 Yin W, Kann K, Yu M, and Schütze H. 2017. Comparative study of cnn and rnn for natural
427 language processing. *arXiv preprint arXiv:170201923*.
- 428 Young T, Peppard P, Palta M, Hla KM, Finn L, Morgan B, and Skatrud J. 1997. Population-based
429 study of sleep-disordered breathing as a risk factor for hypertension. *Archives of internal*

430 *medicine* 157:1746-1752.

431 Zeiler MD, and Fergus R. 2014. Visualizing and understanding convolutional networks. European
432 conference on computer vision: Springer. p 818-833.

433

434

Table 1 (on next page)

Details of our modified LeNet-5 convolutional neural network

Layer	Parameter	Output Shape	Number ^a
Input	—	(None, 900, 2)	0
Conv1	32×5×2, stride 2, pad 0	(None, 448, 32)	352
Max pooling2	3, stride 3, pad 0	(None, 149, 32)	0
Conv3	64×5×2, stride 2, pad 0	(None, 73, 64)	10304
Max pooling4	3, stride 3, pad 0	(None, 24, 64)	0
Dropout5	0.8 rate	(None, 24, 64)	0
FC6	32, relu	(None, 32)	49184
Output	2, softmax	(None, 2)	66

1 ^a The number of parameters generated by the corresponding operation.

2

Table 2 (on next page)

Feature set extracted based on previous studies

Name	Derived from		Details
	RR ^a	Ampl ^b	
RMSSD	×		Square root of the average of the squared difference between adjacent RR intervals.
SDNN	×		Standard deviation of the difference between adjacent RR intervals.
NN50	×		Number of adjacent RR intervals exceeds 50 ms.
pNN50	×		NN50 divides by the number of RR intervals.
Mean RR	×		Mean of RR intervals.
Mean HR	×		Mean of heart rate (HR), which is derived from RR intervals.
Normalized VLF	×	×	Normalized very low frequency (VLF) component of the corresponding signal.
Normalized LF	×	×	Normalized Low frequency (LF) component of the corresponding signal.
Normalized HF	×	×	Normalized high frequency (HF) component of the corresponding signal.
LF/ HF	×	×	The ratio of LF to HF of the corresponding signal.
LF/(LF+HF)	×	×	The ratio of LF to LF+HF of the corresponding signal.
HF/(LF+HF)	×	×	The ratio of HF to LF+HF of the corresponding signal.

1 ^a RR intervals of single-lead ECG signal.

2 ^b Amplitudes of single-lead ECG signal.

3

Table 3 (on next page)

The overall performance of our modified LeNet-5 and traditional machine learning methods in per-segment SA detection

Method	Accuracy (%)	Sensitivity (%)	Specificity (%)	AUC
SVM	81.4	76.9	84.3	0.887
LR	80.8	75.7	84.0	0.884
KNN	77.5	68.1	83.4	0.826
MLP	81.1	71.3	87.2	0.898
LeNet-5	87.6	83.1	90.3	0.950

1

Table 4(on next page)

The overall performance of our modified LeNet-5 and traditional machine learning methods in per-recording classification

Method	Accuracy (%)	Sensitivity (%)	Specificity (%)	AUC	Corr. ^a
SVM	88.6	100.0	66.7	0.978	0.852
LR	88.6	100.0	66.7	0.982	0.841
KNN	82.9	100.0	50.0	0.986	0.845
MLP	85.7	95.7	66.7	0.949	0.814
LeNet-5	97.1	100.0	91.7	0.996	0.943

1 ^a The correlation value between the actual *AHI* and the experimentally determined *AHI*.

2

Table 5 (on next page)

The per-segment SA detection and per-recording classification performance in the UCDDDB database

Classifier	Per-segment			Per-recording			Corr .
	Accuracy (%)	Sensitivity (%)	Specificity (%)	Accuracy (%)	Sensitivity (%)	Specificity (%)	
SVM	70.6	32.7	83.3	92.3	100.0	50.0	0.251
LR	69.6	34.7	81.3	84.6	90.9	50.0	0.107
KNN	66.1	38.1	75.4	84.6	100.0	0.0	0.373
MLP	67.2	38.5	76.8	92.3	100.0	50.0	0.263
LeNet-5	71.8	26.6	86.9	92.3	90.9	100.0	0.624

1

Table 6 (on next page)

Comparison between the per-segment SA detection performance of our modified LeNet-5 and existing works

Reference	Features	Classifier	Accuracy (%)	Sensitivity (%)	Specificity (%)
(Varon et al. 2015)	Feature Engineering	LS-SVM	84.7	84.7	84.7
(Song et al. 2016)	Feature Engineering	HMM-SVM	86.2	82.6	88.4
(Sharma & Sharma 2016)	Feature Engineering	LS-SVM	83.4	79.5	88.4
(Li et al. 2018)	Auto encoder	Decision fusion	83.8	88.9	88.4
Our study	CNN	LeNet-5	87.6	83.1	90.3

1

Table 7 (on next page)

Comparison between the per-recording classification performance of our modified LeNet-5 and existing works

Reference	Classifier	Accuracy (%)	Sensitivity (%)	Specificity (%)	Corr.
(Morillo & Gross 2013)	PNN	93.8	92.4	95.9	—
(Sharma & Sharma 2016)	LS-SVM	97.1	95.8	100	0.841
(Song et al. 2016)	HMM-SVM	97.1	95.8	100	0.860
(Alvarez et al. 2010)	LR	89.7	92.0	85.4	—
(Li et al. 2018)	Decision fusion	100	100	100	—
Our study	LeNe-5t	97.1	100.0	91.7	0.943

1

Figure 1

PhysioNet Apnea-ECG dataset preprocessing scheme. Note: In this study, the labeled segment and its surrounding ± 2 segments of the ECG signal (five 1-minute segments in total) was extracted as a whole for processing.

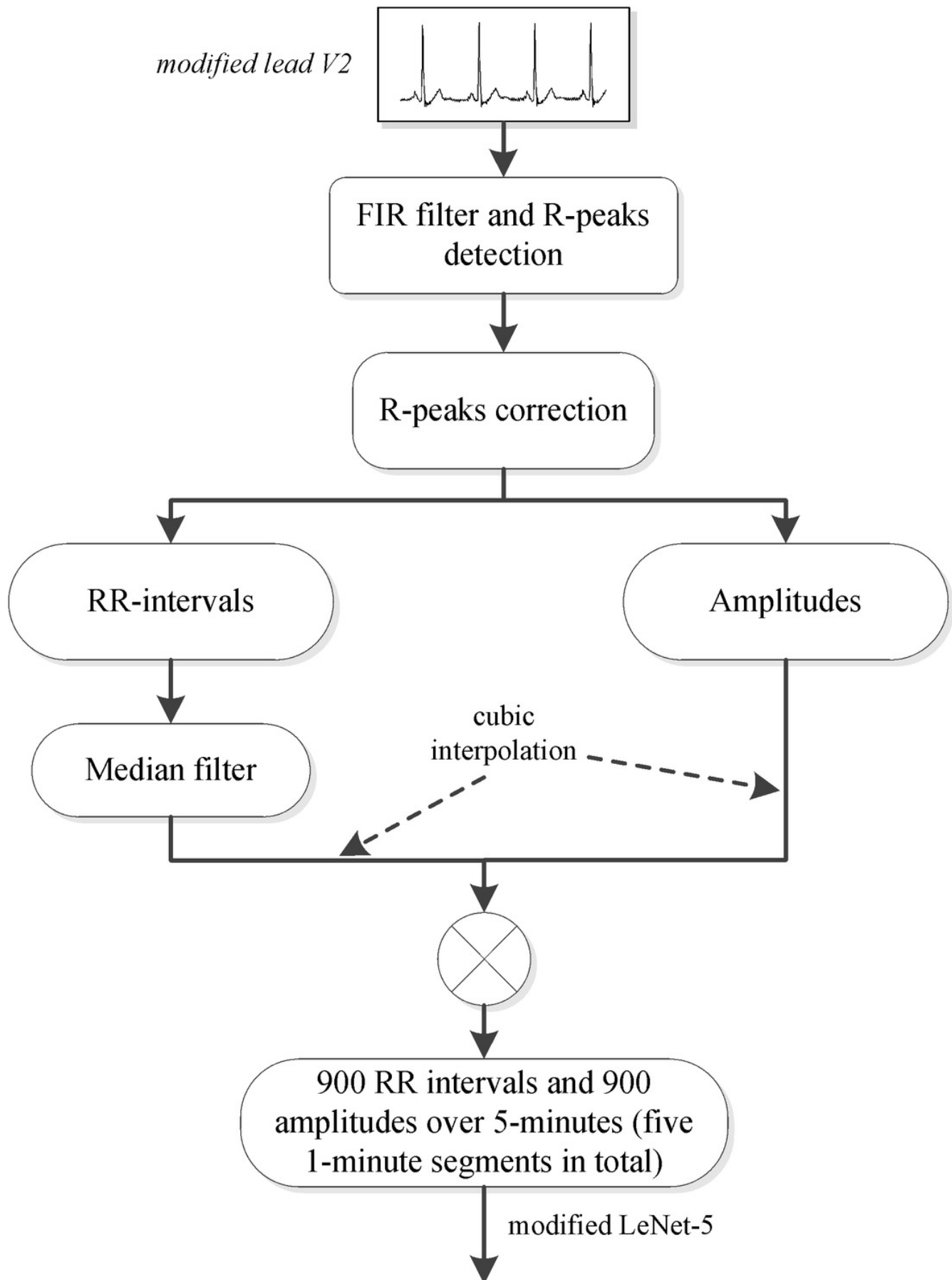


Figure 2

Architecture of our modified LeNet-5. It can be seen as a combination of convolutional neural networks (CNN) for feature extraction and full connection (FC, also known as MLP) as classifier

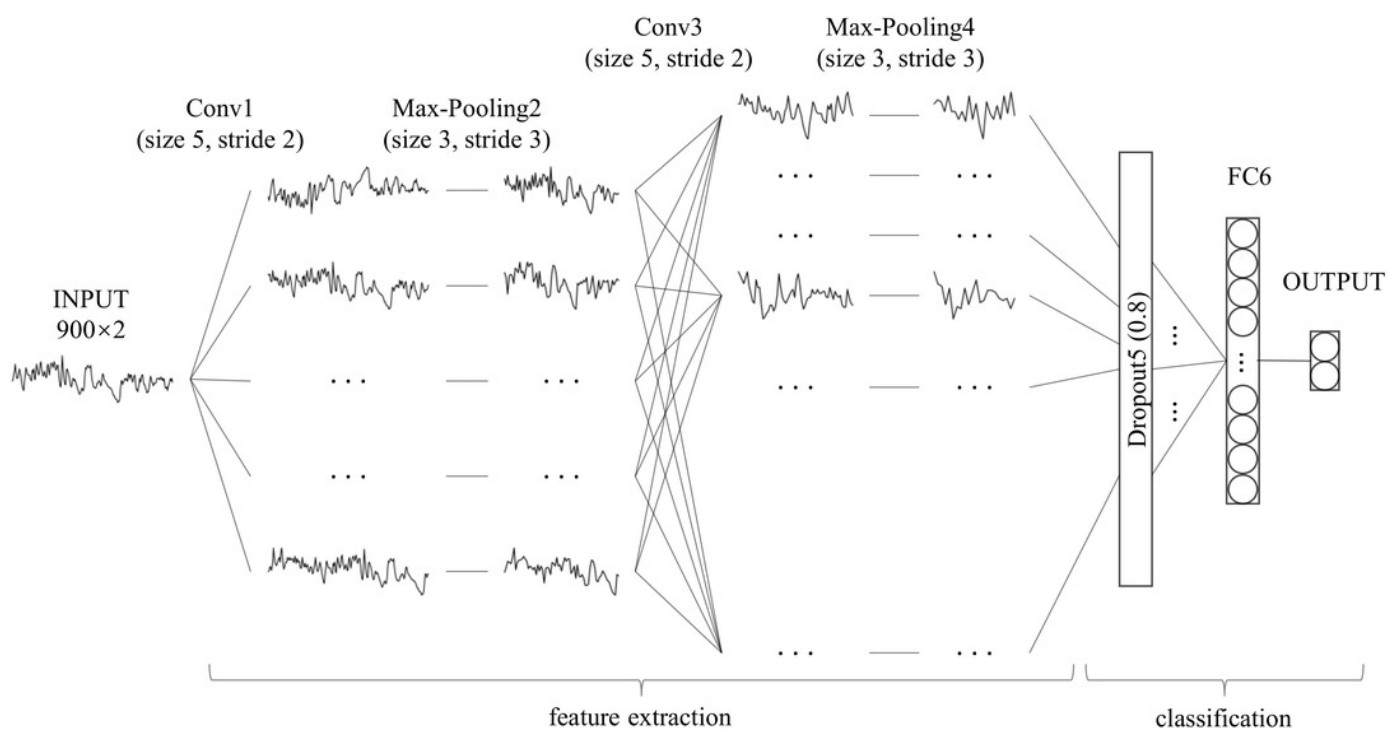


Figure 3

Comparison of ROC curves of our modified LeNet-5 and MLP in per-segment SA detection

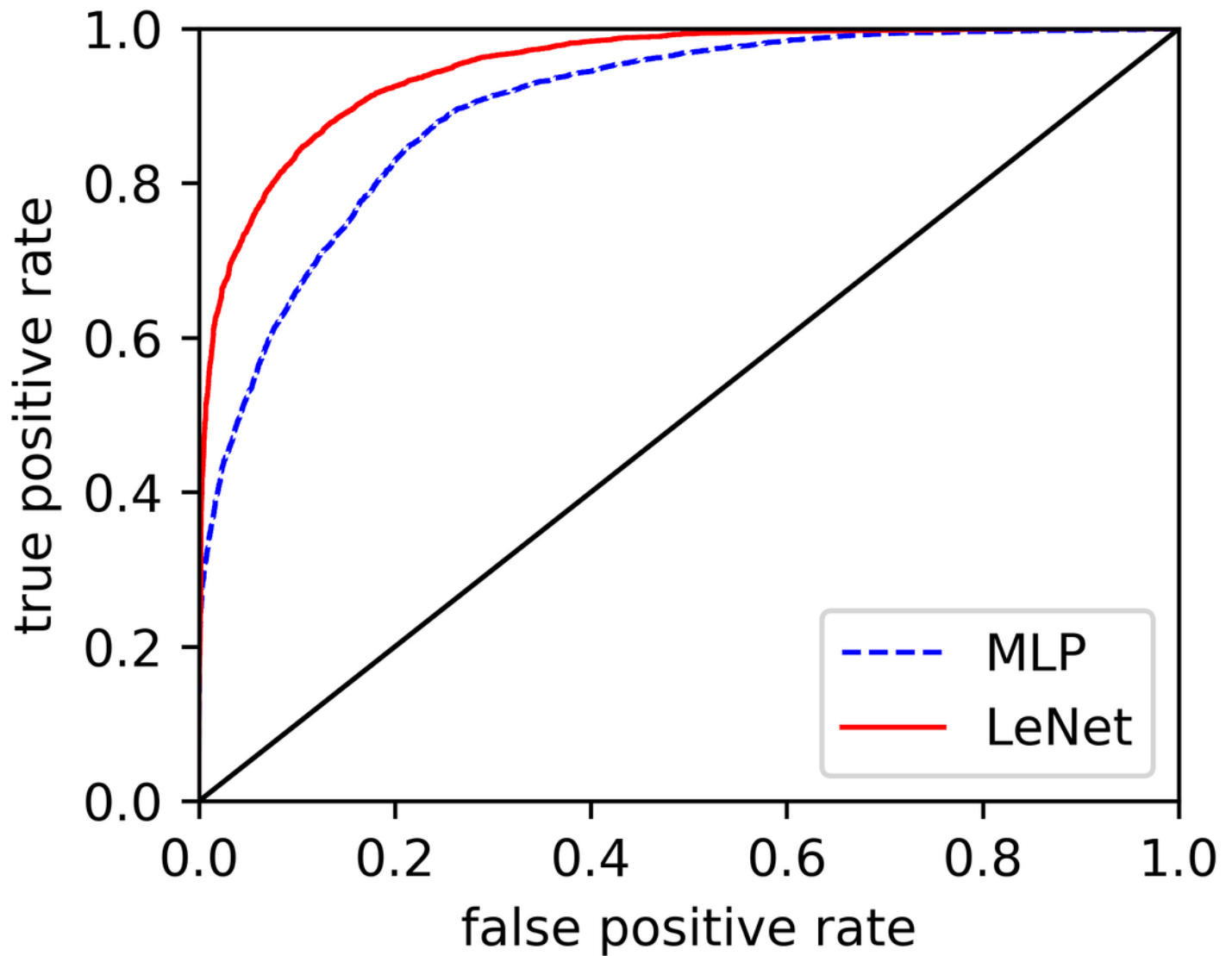


Figure 4

Comparison of the per-segment detection accuracy of five classifiers calculated on 10 different test groups

